Electrochimica Acta 56 (2011) 9637–9643

Contents lists available at ScienceDirect

Electrochimica Acta

journal homepage: www.elsevier.com/locate/electacta

Electroless plating of rhenium–nickel alloys

Alla Duhin[a], Alexandra Inberg[b], Noam Eliaz[a,*,1], Eliezer Gileadi[c,2]

[a] Biomaterials & Corrosion Laboratory, School of Mechanical Engineering & The Materials and Nanotechnologies Program, Tel-Aviv University, Ramat-Aviv, Tel Aviv 69978, Israel
[b] Department of Physical Electronics, Faculty of Engineering, Tel-Aviv University, Ramat-Aviv, Tel Aviv 69978, Israel
[c] School of Chemistry, Faculty of Exact Sciences, Tel-Aviv University, Ramat-Aviv, Tel Aviv 69978, Israel

ARTICLE INFO

Article history:
Received 2 March 2011
Received in revised form 8 May 2011
Accepted 9 May 2011
Available online 18 May 2011

Keywords:
Electroless plating
Rhenium–nickel alloys
Thin film
Induced codeposition

ABSTRACT

In this study, rhenium–nickel (Re–Ni) films were formed by electroless deposition on conductive (Cu) and non-conductive (SiO_2) substrates. Different bath compositions were evaluated, aiming to achieve high Re-content. Both sodium hypophosphite and dimethylamine-borane were used as reducing agents. Films containing up to 75 at% Re were obtained. The influence of nickel concentration in the solution on alloy composition, deposition rate and surface morphology were determined. It is shown that Ni^{2+} acts as a catalyst for the in situ reduction of the perrhenate ion, in a manner similar to what was proposed for electroplating of the same alloy. The rate of electroless plating is similar to that found in electroplating at an applied current density of 50 mA cm^{-2}. While pure Re cannot be deposited from our electroless plating baths, the addition of even a very small amount of Ni^{2+} ions (0.25 mM) is enough to start the induced codeposition of Re. Proper selection of the bath composition can lead to fine control of the alloy thickness and its Re-content, thus making it potentially attractive for thin barrier layers.

1. Introduction

The superior mechanical and physical properties of rhenium make it a very attractive metal for a variety of applications for industries such as aircraft, aerospace, nuclear, electronic, biomedical and catalysis [1–7]. While Re-based alloy coatings have been produced largely by chemical vapor deposition (CVD), and to a lesser extent by electroplating [1,8–10], very little has been reported on electroless deposition of Re and its alloys. The most important advantage of electroless plating is the ability to coat non-conductive surfaces. It is most suitable for the formation of very thin layers, in the range of 10–100 nm, which can be used as the final product or as the basis of thicker layers of the same alloy formed by electroplating. Better uniformity of deposition and better via/trench filling than in the case of electroplating are obtained, because there is no counter electrode in electroless plating, and therefore primary current distribution cannot exist.

Alloys of amorphous Ni–P prepared by electroless deposition are widely used as protective and decorative coatings on various substrates. The effect of addition of $KReO_4$ to a Ni–P electroless plating bath has been studied [11,12]. The alloys produced contained 45 at% Re and 2–3 at% P. It was shown that the Ni–P–Re deposits had a melting point of about 1970 K, nearly twice that of Ni–P films. Mencer [13] investigated Ni–Re–P coatings obtained from an acidic bath. In that case the deposit contained only 3.5 at% of Re. The as-deposited films were amorphous. It was found that the crystallization temperature increased with increasing Re-content of the film. Osaka et al. [14] studied the thermal stability of the Ni–P alloy when NH_4ReO_4 was added to the plating bath. Films with Re-content as high as 50 at% were prepared at pH 8.5–9.0. It was also shown that the thermal stability increased with increasing Re-content in the film. Similar investigation of the Ni–Re–B alloy was performed by Kim et al. [15]. In this case, dimethylamine-borane (DMAB) was used as the reducing agent. The Re-content of the deposited film increased with increasing concentration of the ReO_4^- ion, while the B-content decreased. The as-deposited coatings were amorphous for low Re-content, but a fine devitrified hexagonal close-packed Re–Ni phase was observed for films with a high concentration of Re. Electroless deposition of Ni–Re–P alloys from alkaline citrate solutions was investigated by Valova et al. [16]. The deposited films were amorphous, with Re-content less than 10 at%, and a very homogeneous thickness distribution of all alloy components was observed.

The objective of the current study was to achieve high Re-content in electroless plating of rhenium–nickel (Re–Ni) alloys. Alloys were deposited from an alkaline medium (pH 9.5–10.0), both on conducting and on non-conducting surfaces, and Re-content as high as 75 at% was obtained.

2. Experimental

The different compositions of electrolytes used are listed in Table 1. Potassium perrhenate and nickel sulfate were employed

* Corresponding author. Tel.: +972 3 640 7384; fax: +972 3 640 7617.
E-mail address: neliaz@eng.tau.ac.il (N. Eliaz).
[1] ISE member.
[2] ISE Fellow.

0013-4686/$ – see front matter © 2011 Elsevier Ltd. All rights reserved.
doi:10.1016/j.electacta.2011.05.030

Table 1
Bath compositions (mM) for electroless deposition of Re–Ni alloys.

Bath chemistry	A	B	B′	C	D	D′	E	E′	F	F′
$NiSO_4$	38	19	19	6.3	7.6	7.6	3.8	3.8	3.8	3.8
$KReO_4$	17	34.5	34.5	29	48	48	34.5	34.5	69	69
NaH_2PO_2	190	190	0	190	190	0	190	0	190	0
DMAB	0	0	100	0	0	100	0	100	0	100
[Re]/[Ni]	0.45	1.8	1.8	4.6	6.3	6.3	9	9	18	18

as the source for rhenium and nickel ions, respectively. Sodium citrate (Na_3Cit) was used as a complexing agent. Two reducing agents were employed in different solutions, to compare their suitability in this electroless plating process: sodium hypophosphite (NaH_2PO_2) and dimethylamine-borane ($(CH_3)_2HNBH_3$, DMAB). The concentrations of the reducing agents were those optimized in our laboratory. Baths B, D, E and F have the same composition as B′, D′, E′ and F′, except that the reducing agent is different. The concentration of Na_3Cit was constant at 170 mM in all cases, while the ratio of the two metals in solution was varied. The pH was adjusted to 9.5–10 by adding sodium hydroxide and sometimes hydrochloric acid. The temperature of the bath was maintained at 90–95 °C.

Re–Ni deposits were formed by electroless deposition on three different substrates: pure copper foils, sputtered copper (75 nm) on TaN/SiO_2/Si, and SiO_2 (100 nm)/Si (both commercial wafers from Intel Israel Corporation). All substrates were cleaned and Pd-activated before plating, as described in Table 2. The concentrations of the species in the cleaning and activation processes shown in Table 2 are given in units of relative volumes. The copper substrates were cleaned to remove the oxide layer. Afterwards, all substrates were rinsed in deionized water. Then, the substrates were activated by dipping in Pd-citrate buffer solution (pH 2.5) for 2 min. The SiO_2 (100 nm)/Si substrate was cleaned by RCA (Radio Corporation of America) solutions, as shown in Table 2, in order to remove any organic material (Bath I) and metallic impurities (Bath II).

In order to improve the adhesion of the Re–Ni deposits to the non-conducting SiO_2 substrate, the latter was immersed for 3 h at 50–60 °C in a 1% solution of aminopropyltrimethoxysilane (terminated with an NH_2 group) in ethanol, to form a monolayer of this silane on the surface. Subsequently, the samples were rinsed in ethanol using ultrasonic agitation. After silanization, the substrates were activated in Pd-citrate buffer solution (pH 2.5) for 20 min. All experiments were performed in a 25 mL open beaker containing 10 mL solution (freshly prepared for each experiment), without agitation. The size of all samples was 20 × 20 mm.

The thickness of the Re–Ni film was measured using a Tencor Alpha-Step 500 profilometer (0.1 nm vertical resolution). This was done by measuring a selectively etched step formed on part of the sample. The step etching was conducted in a solution consisting of 1:1:3 HNO_3:HCl:H_2O.

The surface morphology of the deposits after drying was observed by means of an environmental scanning electron microscope (ESEM, Quanta 200 FEG from FEI) operated in the high vacuum mode (thus, the abbreviation SEM will be used below). The attached liquid-nitrogen-cooled Oxford Si EDS detector was used to determine the atomic composition of the alloy. Both the film composition and its thickness were measured at different locations on each of 3 to 5 different samples. Thus, the values are presented in Figs. 1–4 and Fig. 7 as (average ± standard deviation). The chemical composition of selected samples was analyzed using X-ray photoelectron spectroscopy (XPS) measurements, performed in UHV (3.3×10^{-8} Pa base pressure) using 5600 Multi-Technique System (PHI, MN). The samples were analyzed at the surface and during Ar^+ ion-sputtering with 2 kV ion gun (raster: 4 × 4 mm, sputtering rate for SiO_2/Si is 1.6 nm min^{-1}).

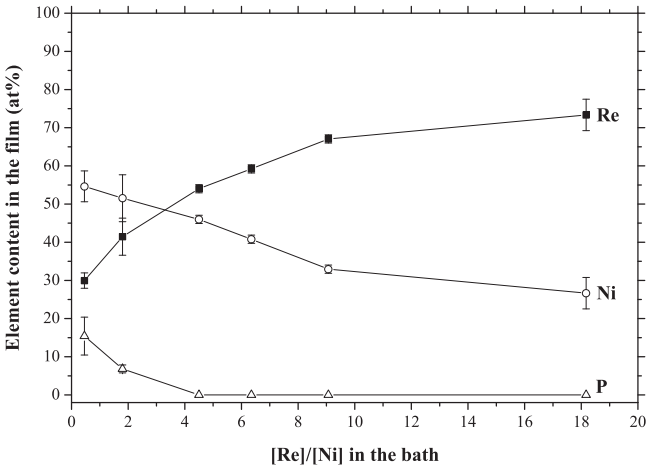

Fig. 1. Rhenium, nickel and phosphorous contents (at%, based on EDS) in the deposit as a function of the [Re]/[Ni] concentration ratio in the bath. NaH_2PO_2 was used as the reducing agent. The films were deposited on Cu (75 nm) on TaN/SiO_2/Si substrate.

The surface topography was studied by an atomic force microscope (AFM, MultiMode, Digital Instruments, Inc., USA). Commercially available Ti-Pt coated/ultra-sharp Si tips produced by MicroMasch, Spain, were used for all measurements. The AFM scanning area was 1 × 1 μm.

3. Results and discussion

3.1. Composition of electroless deposited Re–Ni films

Different bath compositions (Table 1) were evaluated and studied in order to achieve high-quality films with high Re-content. The concentrations of citrate and of the reducing agents were kept con-

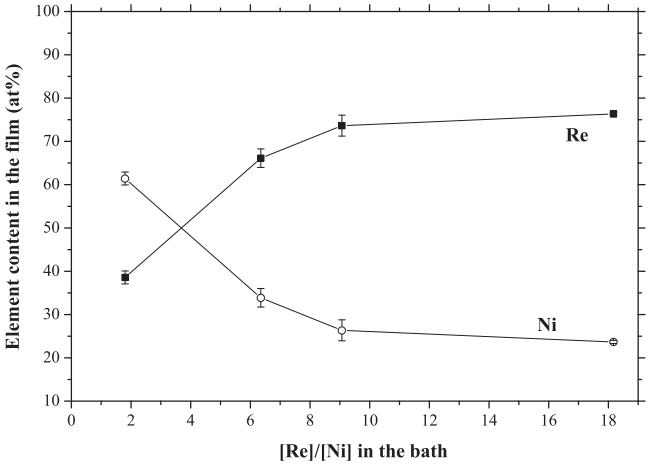

Fig. 2. Rhenium and nickel contents (at%, based on EDS) in the deposit as a function of the [Re]/[Ni] concentration ratio in the bath. DMAB was used as the reducing agent. The films were deposited on Cu (75 nm) on TaN/SiO_2/Si substrate.

Table 2
Pretreatment of the different substrates.

Substrate:	Cu-foil	Cu-sputtered on TaN/SiO_2/Si	SiO_2 (100 nm)/Si
Pre-cleaning conditions	11:4:5 H_3PO_4:HNO_3:CH_3COOH, 60–70 °C, 1 min	1:50 CH_3COOH:H_2O, RT,[a] 2 min	Bath I: 5:1:1 H_2O:NH_4OH:H_2O_2, 60–70 °C, 20 min Bath II: 6:1:1 H_2O:HCl:H_2O_2, 60–70 °C, 20 min
Silanization	–	–	50–60 °C, 3 h
Activation	Pd-citrate, RT,[a] 2 min	Pd-citrate, RT,[a] 2 min	Pd-citrate, RT,[a] 20 min

[a] RT – Room temperature.

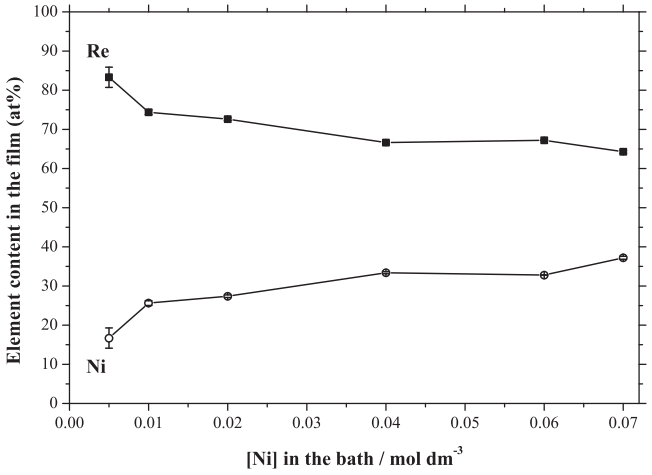

Fig. 3. Rhenium and nickel contents (at%, based on EDS) in Re–Ni coatings as a function of Ni concentration in solution. The concentrations of $KReO_4$, Na_3Cit and DMAB in the bath were 69, 170 and 100 mM, respectively, and pH 9.5. The films were deposited on Cu (75 nm) on TaN/SiO_2/Si substrate.

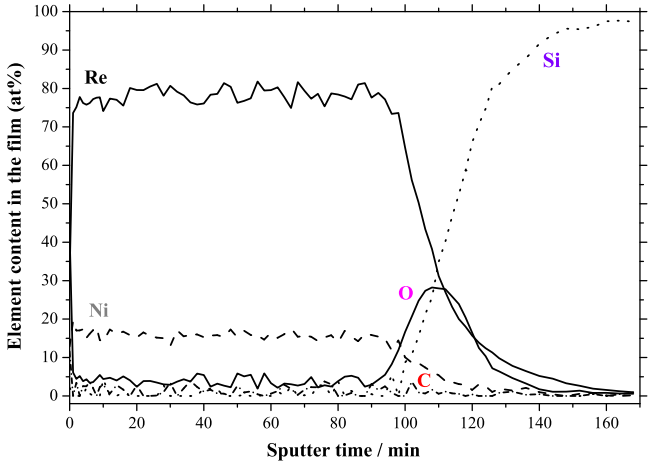

Fig. 5. The XPS depth profile of a Re–Ni alloy deposited from bath E′ (Table 1) on SiO_2 (100 nm)/Si substrate. The sputtering rate was about 1.6 nm min^{-1} up to 80 min, and 2.5 nm min^{-1} after that.

stant in all baths, while the concentrations of ReO_4^- and of Ni^{2+} were changed.

As expected, the ratio of concentrations of the two metals in the deposited alloy depends on the composition of the solution, as shown in Figs. 1 and 2. In Fig. 1, the Re-content in the film is seen to increases from 30 at% to 67 at% as the [Re]/[Ni] concentration ratio in the bath is raised from 0.5 to 9. A further increase of this ratio to 18 leads to a relative small increase in the concentration of Re in the alloy (to 73 at%), indicating that a saturation value is approached. Up to a ratio of about [Re]/[Ni] ≤ 5 in solution, some phosphorous is found in the alloy, but beyond that the alloy contains only Re and Ni.

A similar behavior was observed when DMAB was used as the reducing agent, as shown in Fig. 2. The Re-content in the film increases from 38 at% to 73 at% as the [Re]/[Ni] concentration ratio in the bath is raised from 2 to 9. Further increase of the [Re]/[Ni] ratio in the solution has only a moderate effect on Re concentration in the film, raising it to 76 at%. However, in this case, no boron was observed in the deposits (but, one should note the typically low

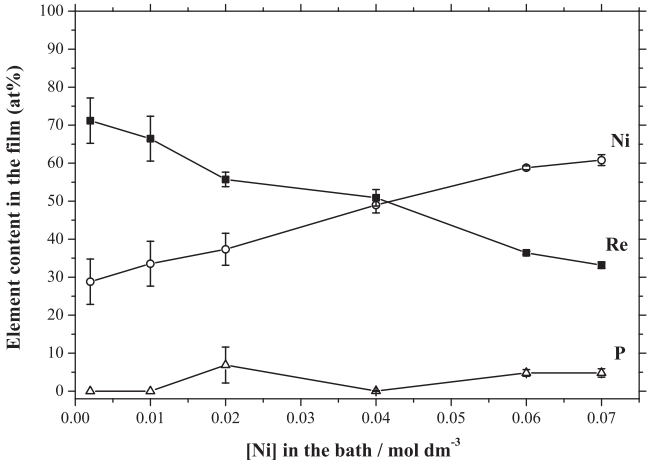

Fig. 4. Rhenium, nickel and phosphorus contents (at%, based on EDS) in Re–Ni coatings as a function of Ni concentration in the solution. The concentrations of $KReO_4$, Na_3Cit and NaH_2PO_2 in the bath were 69, 170 and 190 mM, respectively, and pH 9.5. The films were deposited on Cu (75 nm) on TaN/SiO_2/Si substrate.

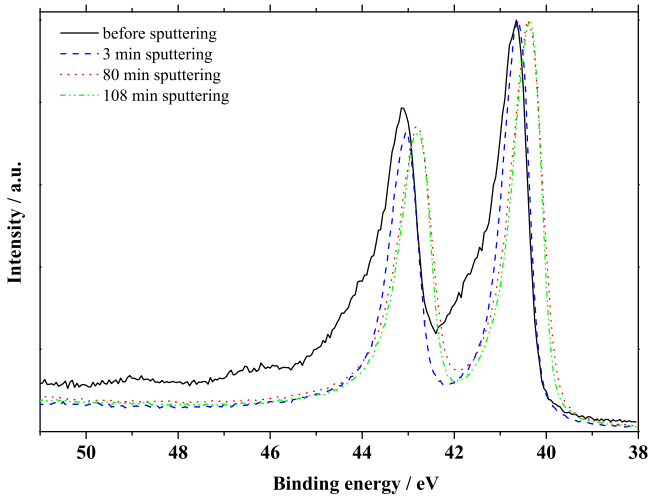

Fig. 6. High-resolution XPS spectra, showing the position of the Re4f peaks.

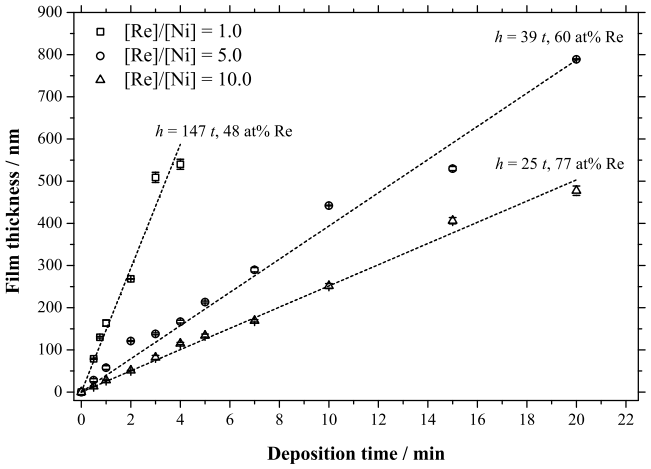

Fig. 7. The thickness of Re–Ni layers deposited from a solution containing 34.5 mM ReO_4^- as a function of the deposition time. The three lines correspond to different Re-contents in the alloys, as marked in the figure along with the slope (deposition rate) values.

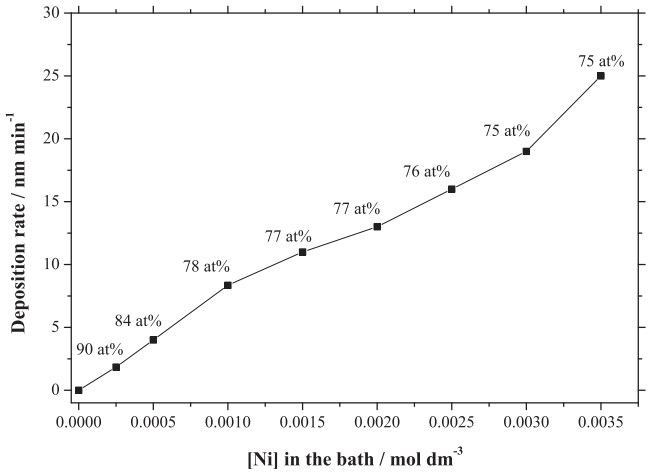

Fig. 8. Deposition rate of Re–Ni alloys as a function of the concentration of Ni in solution containing 34.5 mM ReO_4^-. The substrate was Cu (75 nm) on TaN/SiO_2/Si.

sensitivity of EDS to boron). In both cases, the curves for Re- and Ni-content crossed when the ratio of metal ions in solution was [Re]/[Ni] = 3. This is, of course, the point where the deposited alloy contains equal atomic concentration of the two metals. At the highest [Re]/[Ni] ratio in solution, their ratio in the alloy increased to 2.70 and 3.17 when hypophosphite and DMAB were used, respectively (Figs. 1 and 2).

As seen in Figs. 1, 2 and in Table 1, there is almost no difference in the Re-content of the film as the ratio of [Re]/[Ni] in solution is increased from 9 to 18. Considering that the perrhenate salt is much more expensive than the Ni salt, baths E and E′ in Table 1 should be preferred over baths F and F′. The effect of the concentration of Ni^{2+} in solution, holding the concentration of ReO_4^- constant at 69 mM and using DMAB as the reducing agent, is shown in Fig. 3. A similar experiment, but employing hypophosphite, is shown in Fig. 4. Beyond a concentration of 20 mM Ni^{2+} (corresponding to a ratio of [Re]/[Ni] = 3.45), the Re-content in the deposit is about 65 at%, almost independent of the concentration of Ni^{2+}, until the [Re]/[Ni] ratio in solution reaches a value of unity. Note that in this case, the concentration of Re in the alloy is higher than that of nickel over the whole range of concentrations of the latter in solution.

When NaH_2PO_2 is used as a reducing agent, the Re-content in the alloy decreases monotonically from 73 at% to 34 at% as the concentration of Ni^{2+} in solution is increased, as shown in Fig. 4. The composition of the alloys produced by electroless plating depends also on the reducing agents employed. DMAB and NaH_2PO_2 have been reported to incorporate some boron and phosphorus, respectively. In the current study, a small amount of phosphorous was detected in coatings at lower ratios of [Re]/[Ni] in the solution, but no incorporation of boron was observed in any of the baths tested.

Based on the data shown in Figs. 1–4 it can be concluded that DMAB is a somewhat better reducing agent than NaH_2PO_2, under the conditions tested here, because it can yield alloys having a higher Re-content and free of a third element (in this case, boron).

The Re–Ni alloy films with high Re-content were also deposited on electrically insulating SiO_2 substrate, which is a very common dielectric material in microelectronics technology. The composition of Re–Ni films on SiO_2/Si substrates was evaluated using XPS technique. The depth profile of a Re–Ni alloy deposited from bath E′ ([Re]/[Ni] = 9) with DMAB as the reducing agent is shown in Fig. 5. The distribution of Re and Ni across the depth profile of the film is uniform. The film consists mostly of 75–80 at% Re. The Ni-content is about 15–17 at%. In addition, a small amount of oxygen (about 4 at%) was found. The atomic composition of rhenium and nickel as well as the absence of boron in the alloy characterized by XPS are very close to those determined by EDS (Fig. 2), using the same bath composition (bath E′, Table 1). This shows that it is possible to obtain by electroless plating boron-free, high Re-content alloys, which is required for thin film barrier layers in microelectronics and other applications.

The HRXPS spectrum was analyzed to evaluate the incorporation of oxides (if any) into the Re–Ni deposits (Fig. 6). The position of the Re4f peaks was characterized before and after sputtering. The position of the peaks before sputtering (40.65 eV and 43.15 eV) hardly changed after 3 min sputtering (40.60 eV and 43.05 eV, respectively), but was significantly changed after 80 min sputtering (40.40 eV and 42.80 eV, respectively). Further sputtering, up to 108 min, had only a minor effect on the peak position (40.35 eV and 42.75 eV, respectively). Thus, it is evident that the oxidized state of Re exists only at the surface (c.f. Fig. 5).

Table 3
Surface roughness at different stages of surface modification, as measured by AFM.

Surface	Roughness (Z_{RMS})/nm
Sputtered Cu (75 nm) on TaN/SiO_2/Si substrate	0.70 ± 0.05
Cu substrate after cleaning	0.90 ± 0.10
Cu substrate after Pd-citrate activation	1.81 ± 0.20
Re–Ni alloy deposited from a bath with [Re]/[Ni] = 1	2.00 ± 0.10
Re–Ni alloy deposited from a bath with [Re]/[Ni] = 5	2.50 ± 0.30
Re–Ni alloy deposited from a bath with [Re]/[Ni] = 10	3.50 ± 0.50

3.2. Deposition rate

The thickness dependence of electroless plated Re–Ni alloys on deposition time is presented in Fig. 7. Substrates of copper (75 nm) on TaN/SiO_2/Si were used for these measurements, because it was essential to use highly polished surfaces. The thicknesses of the layers were measured by alpha-step, using selective etching for step formation on part of the sample. In order to estimate the error in the thickness measurements, 3–5 samples were analyzed for each deposition time. The Re–Ni alloys were deposited from a bath containing 34.5 mM ReO_4^-, with DMAB as the reducing agent. The concentration of Ni^{2+} was varied in order to obtain molar ratios of [Re]/[Ni] = 1, 5 and 10 in the plating bath.

The film deposition rate is reduced from 147 to 39 and to 25 nm min^{-1} as the [Re]/[Ni] ratio in the solution is increased from 1 to 5 to 10, i.e. as the concentration of Ni in the bath is reduced and the Re-content of the alloy is increased, as evident in Fig. 7.

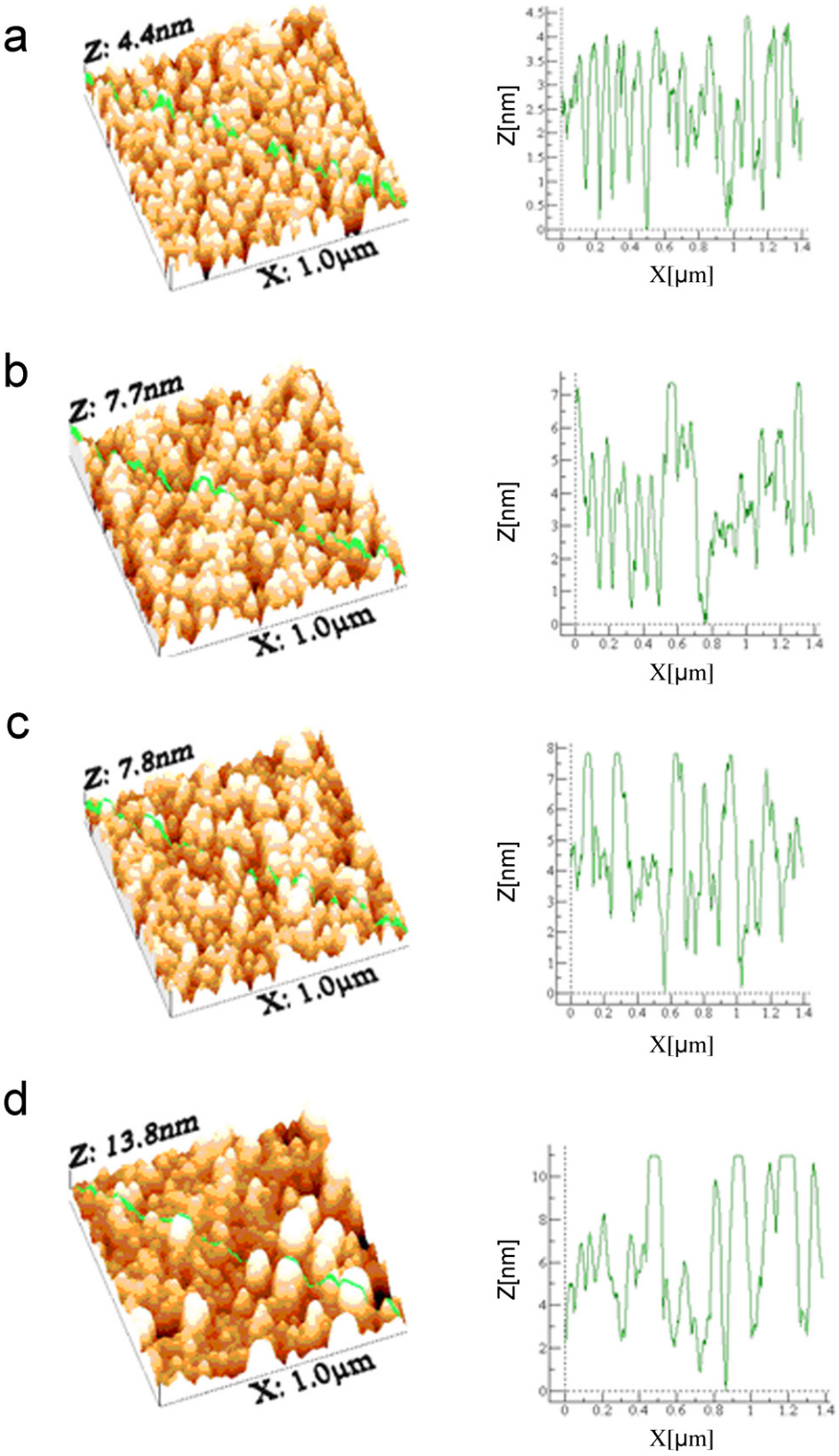

Fig. 9. AFM images of the surfaces of: (a) the Cu (75 nm) on TaN/SiO_2/Si substrate, and (b–d) 160 ± 10 nm thick Re–Ni films grown on it. The film deposition rate (nm min^{-1}) and [Re]/[Ni] molar ratios were, correspondingly: 147, 1.0 (b); 39, 5.0 (c); 25, 10.0 (d).

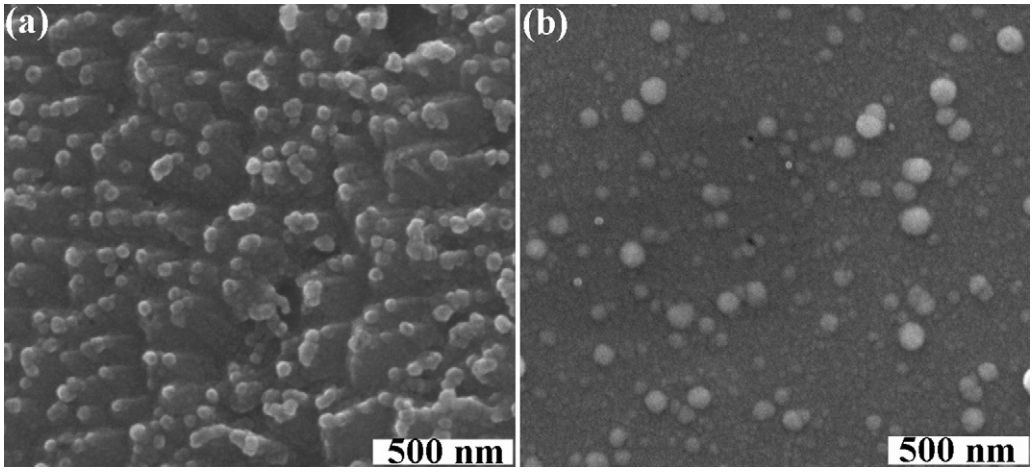

Fig. 10. SEM images of Re–Ni films deposited on: (a) Cu-foil, and (b) SiO_2/Si substrates from a bath with [Re]/[Ni] = 10.0. Film thickness: 160 ± 10 nm.

In a solution with [Re]/[Ni] = 1, reduction of the metals in the bulk of the solution was observed after about 4 min. Therefore, the deposition time in this solution was limited to 4 min.

3.3. Deposition from solutions containing a very low concentration of Ni

The results presented in Figs. 2, 3 and 7 clearly show that reducing the concentration of Ni^{2+} ions in the bath results in an increase in the Re-content in the deposit, as expected. Thus, it was of interest to analyze the electroless plating process in solutions containing very little Ni^{2+}, or no Ni^{2+} at all. The dependence of the deposition rate of the film in this region, using DMAB as a reducing agent, is shown in Fig. 8.

A significant increase in the rate of deposition was observed already when the Ni^{2+} concentration in the bath increased from 0.25 mM to 3.5 mM (corresponding to [Re]/[Ni] concentration ratio of 138–10). On the other hand, the Re-content in the deposits decreased from 85 ± 3 at% to 77 ± 2 at% when the Ni^{2+} concentration in the solution was increased above 0.5 mM, due to the increased rate of Ni deposition. It is also noted that the deposition rates observed extrapolate to zero when the concentration of Ni^{2+} is zero. This result, combined with the fact that pure Re could not be deposited by electroless plating in our system, shows that Ni^{2+} in solution acts as a catalyst for the reduction of ReO_4^-. This conclusion is in agreement with previous investigations [8,9] where a catalytic effect of Ni on the Re–Ni electroplating process was found.

It is shown in Fig. 8 that even a very small amount of nickel in the electrolyte initiates the reaction, and a Re–Ni film is formed. The deposition rates in these cases are very low (about 4 nm min^{-1}), but this could be an advantage when deposition of a very thin layer of Re–Ni alloy is required, for example as a barrier layer.

3.4. Surface morphology

The Re–Ni film surface topography was studied by AFM. Measurements were performed on the same copper sample that underwent each of the surface modification steps in order to observe the surface transformation. Sputtered Cu (75 nm) on TaN/SiO_2/Si substrates was used for this characterization. The results of the roughness (Z_{RMS}) measurements are summarized in Table 3. AFM images of Cu substrate and 160 nm Re–Ni films plated at different deposition rates from different solutions (cf. Fig. 7) are presented in Fig. 9.

As seen in Table 3, the Cu substrate is very flat, with relatively low Z_{RMS} value. After cleaning, the surface roughness slightly increases to 0.9–1.0 nm (Fig. 9a). A significant increase of the Z_{RMS} value is observed following activation with Pd. Deposition of 160 nm thick Re–Ni alloy increases the roughness a little bit when the rate of film deposition is higher than 40–45 nm min^{-1} and the Re-content does not exceed 60 at% (Figs. 9 b and c). Re–Ni films with higher Re-content (>70 at%) plated at a rate of about 26 nm min^{-1} demonstrated a rougher corrugated surface (Fig. 9d). The deposition of the rough and corrugated coatings in electroless plating is usually caused by a high deposition rate; therefore, this effect could most likely be explained by the different rate of alloy formation under applied process conditions (Fig. 7). We have not studied yet in detail the microstructure of the alloys prepared in this work. However, Kim et al. [15] have reported that Ni–Re–B films with high Re-content exhibit fine crystalline structure, which may be responsible for the low roughness of films with Re-contents lower than 60 at%. Increasing the Re-content in the alloy to above 70 at% seems to allow the formation of a more clustered, rough surface morphology.

SEM study of Re–Ni alloys deposited on different substrates was also conducted. The Re–Ni alloys were deposited from bath E′ (Table 1). The morphology of the films plated on Cu foil (Fig. 10a) and on SiO_2/Si substrates (Fig. 10b) was compared. It is evident that Re–Ni deposit on SiO_2/Si shows a smoother and denser structure than that on Cu. Furthermore, several large clusters are visible on the smooth surface (Fig. 10b).

AFM and SEM observations showed that the surface morphology of electroless deposited Re–Ni alloys strongly depends on the rate of film deposition (cf. Fig. 9), which in turn depends on the bath composition, as discussed above. It also depends on the substrate material and the quality of its surface.

4. Conclusions

Rhenium–nickel alloys with high Re-content (>75 at%) were deposited on conductive (Cu) and non-conductive (SiO_2) substrates. Pure Re could not be deposited by electroless plating, hence Ni^{2+} was added to the plating baths in order to catalyze the deposition of Re.

The kinetics of Re–Ni film deposition from solutions containing different concentrations of Ni^{2+} and different ratios of [Re]/[Ni] in solution was studied. Strong dependence of film deposition rate and Re–Ni alloy composition on the [Re]/[Ni] ratio in solution was observed.

The surface morphology of the Re–Ni films was investigated and found dependent on bath composition as well as on the substrate material.

The mechanism proposed earlier in our laboratory for the catalytic effect of Ni^{2+} in solution on the rate of electrodeposition of Re–Ni alloys and on the high concentration of Re in the deposited alloy [8–10] seems to apply also in the case of electroless deposition. In particular, it is noted that in both plating methods one can readily obtain alloys in which the at% of Re exceeds that of Ni. This is in stark contrast to the induced codeposition of W with Ni, where it is difficult to obtain W-content of 50 at%, showing that the mechanism of induced codeposition must be very different for W and for Re [1,17–21].

In view of the similarities between the behavior observed for electrolytic and electroless deposition, it is most likely that it will also be possible to deposit Re–Co and Re–Fe films by similar electroless procedures.

Two reducing agents were evaluated: sodium hypophosphite and dimethylamine-borane (DMAB). Catalytic deposition of Re was found in both cases, but the latter yielded somewhat higher concentrations of Re in the alloy. More importantly, when DMAB was used as the reducing agent, no boron was found in the deposited alloy. In contrast, when sodium hypophosphite was used, phosphorus was detected in the deposit for certain ReO_4^- and Ni^{2+} concentrations.

The deposition rate varied between 25 and 147 nm min^{-1} for [Re]/[Ni] = 10 and 1, respectively. These correspond to average current densities of approximately 2.2 and 13 mA cm^{-2}, respectively (it is hard to calculate the exact current density because in doing so one has to assume that the density of the film is equal to the density of the bulk alloy, and that the latter is a linear combination of the densities and concentrations of the two alloying elements, both assumptions being only approximately correct). These values are similar to those obtained during electroplating at an applied current density of 50 mA cm^{-2} and a Faradaic efficiency of about 50%, for example.

Although, in general, one would like to find a bath in which plating is fast, the low rate of 4 nm min^{-1} shown in Fig. 8 may be useful when deposition of a very thin layer is necessary, particularly since this happens when the concentration of ReO_4^- in solution is high, leading to a high concentration of Re in the alloy.

The electroless plated films hold a great potential to be used as seed layers on non-conducting substrates prior to electroplating of Re-base alloys, or as barrier layers and wear resistant coatings in microelectromechanical systems (MEMS).

Acknowledgements

The authors acknowledge financial support from the US Air Force Office of Scientific Research (AFOSR, grant number FA9550-10-1-0520). We also thank Dr. Larisa Burstein from the Wolfson Applied Materials Research Center at Tel-Aviv University for her help in XPS characterization.

References

[1] N. Eliaz, E. Gileadi, Induced codeposition of alloys of tungsten, molybdenum and rhenium with transition metals, in: C.G. Vayenas, R.E. White, M.E. Gamboa-Aldeco (Eds.), Modern Aspects of Electrochemistry, vol. 42, Springer, New York, 2008, p. 191 (chapter 4).
[2] A. Naor, N. Eliaz, E. Gileadi, S.R. Taylor, The AMMTIAC Quarterly 5 (2010) 11.
[3] S.R. Agnew, T. Leonhardt, JOM 55 (2003) 25.
[4] Yu.N. Gornastyrev, M.I. Katsnelson, G.V. Peschanskikh, A.V. Trefilov, Phys. Status Solidi B 164 (1991) 185.
[5] J.G. Donaldson, F.W. Hoerltel, A.A. Cochran, J. Less Common Metals 14 (1968) 93.
[6] P. Lipetzky, JOM 54 (2002) 47.
[7] C.S. Bob, C.P. Lungu, I. Mustata, L. Frunza, J. Appl. Phys. 41 (2008) 1.
[8] A. Naor, N. Eliaz, E. Gileadi, Electrochim. Acta 54 (2009) 6028.
[9] A. Naor, N. Eliaz, E. Gileadi, J. Electrochem. Soc. 157 (2010) D422.
[10] A. Naor, N. Eliaz, L. Burstein, E. Gileadi, Electrochem. Solid-State Lett. 13 (2010) D91.
[11] A. Duhin, Y. Sverdlov, Y. Feldman, Y. Shacham-Diamand, Electrochim. Acta 54 (2009) 6036.
[12] G.O. Mallory, J.B. Hajdu (Eds.), Electroless Plating: Fundamentals and Applications, American Electroplaters and Surface Finishers Society, Orlando, FL, 1990.
[13] D. Mencer, J. Alloys Compd. 306 (2000) 158.
[14] T. Osaka, N. Takano, T. Kurokawa, K. Ueno, Electrochem. Solid-State Lett. 5 (2002) C7.
[15] M. Kim, T. Yokoshim, T. Osaka, J. Electrochem. Soc. 148 (2001) C753.
[16] E. Valova, S. Armianov, A. Franquet, A. Hubin, O. Steenhaut, J.L. Delplancke, J. Vereecken, J. Appl. Electrochem. 31 (2001) 1367.
[17] O. Younes, E. Gileadi, Electrochem. Solid-State Lett. 3 (2000) 543.
[18] O. Younes, L. Zhu, Yu. Rosenberg, Y. Shacham-Diamand, E. Gileadi, Langmuir 17 (2001) 8270.
[19] O. Younes, E. Gileadi, J. Electrochem. Soc. 149 (2002) C100.
[20] T.M. Sridhar, N. Eliaz, E. Gileadi, Electrochem. Solid-State Lett. 8 (2005) C58.
[21] N. Eliaz, T.M. Sridhar, E. Gileadi, Electrochim. Acta 50 (2005) 2893.